Trial of Brain Redox Imaging and Estimation of Radiation-Induced Redox Change in Mouse Brain

Ken-ichiro Matsumoto,[1] Mizuki Nakamura,[1] Megumi Ueno,[1] Ikuo Nakanishi,[1] Tadashi Kamada,[2] Ken-ichi Yamada,[3] Ichio Aoki[4]

1. Quantitative RedOx Sensing Team, Department of Basic Medical Sciences for Radiation Damages, National Institute of Radiological Sciences, National Institutes for Quantum and Radiological Science and Technology.
2. Clinical Research Cluster, National Institute of Radiological Sciences, National Institutes for Quantum and Radiological Science and Technology.
3. Department of Bio-functional Science, Faculty of Pharmaceutical Sciences, Kyushu University.
4. Functional and Molecular Imaging Team, Department of Molecular Imaging and Theranostics, National Institute of Radiological Sciences, National Institutes for Quantum and Radiological Science and Technology.

Abstract

The *in vivo* T_1-weighted contrasting abilities and signal decay behaviors of several nitroxyl contrast agents, which have been used as redox responsive contrast agents in several magnetic resonance-based imaging modalities, in mouse brain were compared. In addition, daily variations of redox behavior in mouse brain after irradiation of X-ray or carbon-ion beams (C-beam) were tried to estimate based on the *in vivo* reduction rate of amphiphilic nitroxyl contrast agents.

Injection solutions of five types of five-membered-ring nitroxyl contrast agents, i.e. 3-carboxy-2,2,5,5-tetramethylpyrrolidine-*N*-oxyl (CxP), 3-carbamoyl-2,2,5,5-tetramethylpyrrolidine-*N*-oxyl (CmP), 3-methoxy-carbonyl-2,2,5,5-tetramethylpyrrolidine-*N*-oxyl (MCP), acetoxymethyl-2,2,5,5-tetramethylpyrrolidine-*N*-oxyl-3-carboxylate (CxP-AM), and 4-(*N*-methylpiperidine)-2,2,5,5-tetramethylpyrroline-*N*-oxyl (23c), and a six-membered-ring nitroxyl contrast agent, i.e. 4-hydroxyl-2,2,6,6-tetramethylpiperidine-*N*-oxyl (TEMPOL), were prepared. The nitroxyl contrast agent was i.v. injected to a mouse through tail vein. Then, the distributions and pharmacokinetics of nitroxyl contrast agents were compared based on the time course of T_1-weighted MRI. The MRI experiments using CMP or TEMPOL were repeated for mice irradiated by X-ray or C-beam to their head on several deferent timings, i.e. 1, 2, 4, 8 day(s) after irradiation. C-beam was irradiated at Heavy-Ion Medical Accelerator in Chiba (HIMAC, National Institute of Radiological Sciences/ National Institutes for Quantum and Radiological Science and Technology).

The blood-brain-barrier (BBB)-impermeable CxP could not be distributed in the brain. The slightly lipophilic CmP showed slight distribution only in the ventricle, but not in the medulla and cortex. The amphiphilic MCP and TEMPOL had good initial uniform distribution in the brain and showed typical 2-phase signal decay profiles. A brain-seeking nitroxyl probe, CxP-AM, showed an accumulating phase, and then its accumulation was maintained in the medulla and ventricle regions, but not in the cortex. The lipophilic 23c was well distributed in the cortex and medulla, but slightly in the ventricle, and showed relatively rapid linear signal decay.

Decay rates of MCP in mouse brain after irradiation of 8 Gy X-ray, 8 Gy C-beam or 16 Gy C-beams did not show marked clear changes, however relatively little decreasing were observed at day 1 and day 2 after irradiation. Decay rates of TEMPOL was increased 1 after irradiation then gradually recovered to the control level. MCP and TEMPOL showed opposite responses but the timing of redox change may be 1 or 2 days after irradiation.

Nitroxyl contrast agents equipped with a suitable lipophilic substitution group could be BBB-permeable functional contrast agents. MR redox imaging, which can estimate not only the redox characteristics but also the detailed distribution of the contrast agents, is a good candidate for a theranostic tool. Irradiation of ionized radiation to head could cause alternation of redox status in the brain. Detail of redox mechanisms were still in progress.

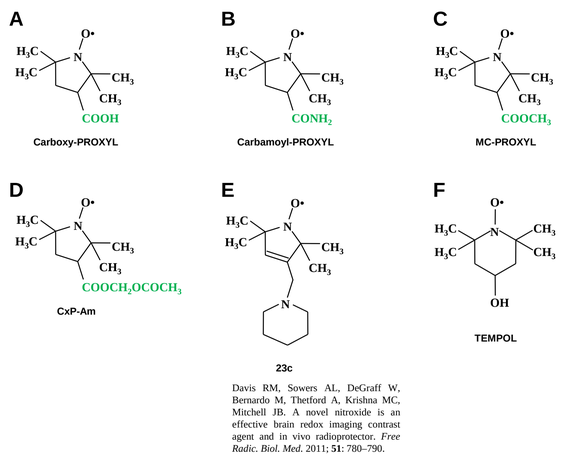

Davis RM, Sowers AL, DeGraff W, Bernardo M, Thetford A, Krishna MC, Mitchell JB. A novel nitroxide is an effective brain redox imaging contrast agent and in vivo radioprotector. *Free Radic. Biol. Med.* 2011; **51**: 780–790.

Fig. 1. Structures of nitroxyl contrast agents. (A) CxP, (B) CmP, (C) MCP, (D) CxP-AM, (E) 23c, and (F) TEMPOL were tested. Substitutional groups on the five-membered ring, i.e. pyrrolidine (A–D) and pyrroline (E), and six-membered ring, i.e. piperidine (F), derivatives determine the lipophilicity and *in vivo* distribution of these contrast agents.

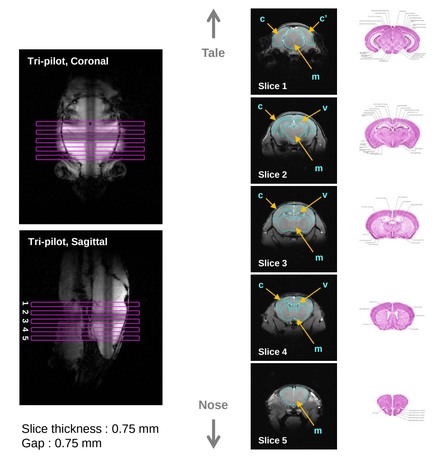

Fig. 2. Position of slices and the scout T_1-weighted images and ROIs. ROI-m, -c, and -v were set up on the regions of the medulla, cortex, and ventricle.

Dyed brain slice images were from http://www.hms.harvard.edu/research/brain/atlas.html

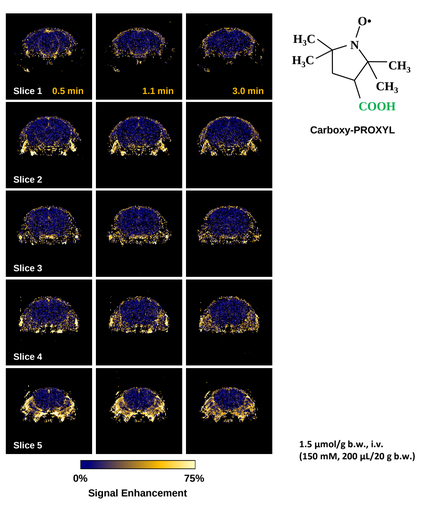

Fig. 3. Distributions of CxP in mouse brain. Vertical columns showed different slices of brain. Horizontal row showed the time course of the T_1-weighted signal enhancement.

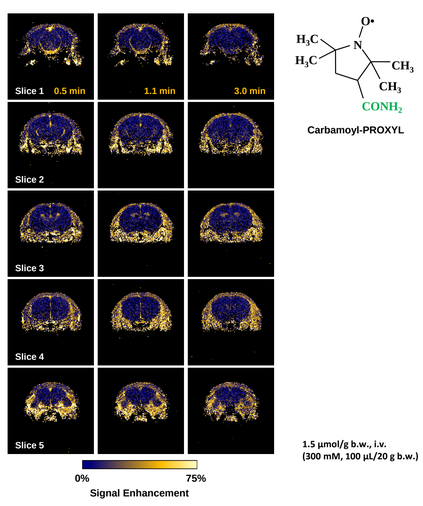

Fig. 4. Distributions of CmP in mouse brain. Vertical columns showed different slices of brain. Horizontal row showed the time course of the T_1-weighted signal enhancement.

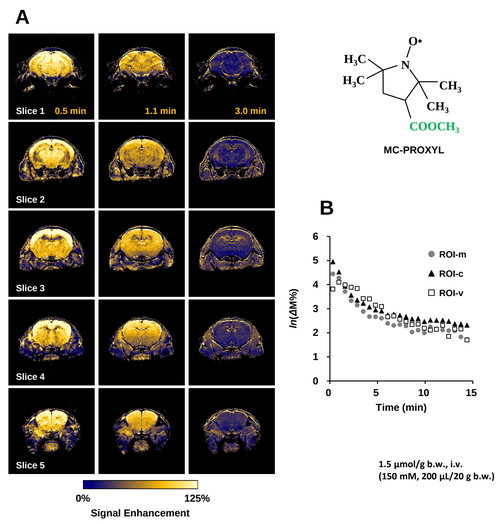

Fig. 5. Dynamic imaging of MCP-induced T_1-contrast. (A) Distributions of MCP in mouse brain and the time course. Vertical columns showed different slices of brain. Horizontal row showed the time course of the MCP-induced T_1-signal enhancement. (B) Time course profiles of MCP-induced signal in brain regions. Profiles indicated by black triangles, gray circles, and open squares were obtained for ROI-c, -m, and -v defined on slice 3, respectively. Values are indicated by average ± SD of 3 mice.

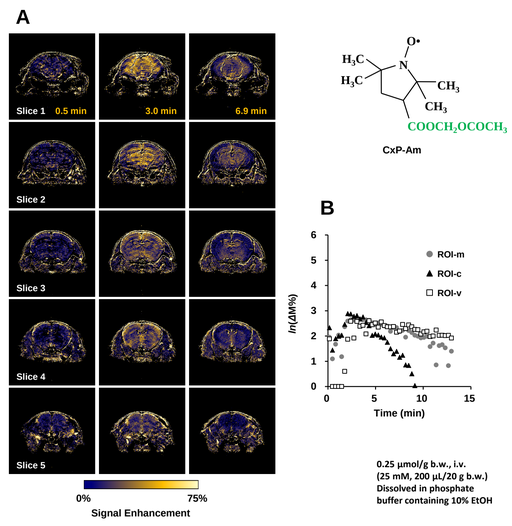

Fig. 6. Dynamic imaging of CxP-Am-induced T_1-contrast. (A) Distributions of CxP-Am in mouse brain and the time cours. Vertical columns showed different slices of brain. Horizontal row showed the time course of the CxP-Am-induced T_1-signal enhancement. (B) Time course profiles of CxP-Am-induced signal in brain regions. Profiles indicated by black triangles, gray circles, and open squares were obtained for ROI-c, -m, and -v defined on slice 3, respectively. Values are indicated by average ± SD of 2 mice.

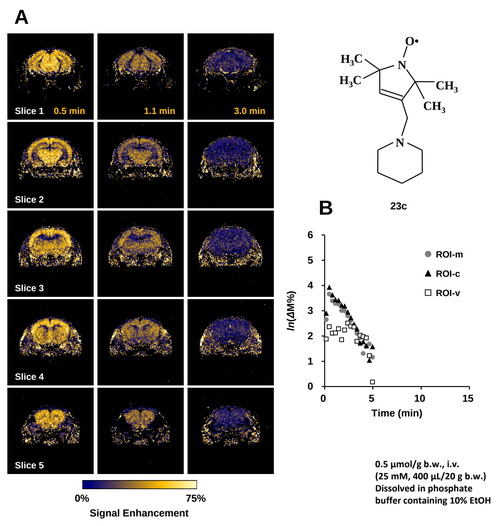

Fig. 7. Dynamic imaging of 23c-induced T_1-contrast. (A) Distributions of 23c in mouse brain and the time course. Vertical columns showed different slices of brain. Horizontal row showed the time course of the 23c-induced T_1-weighted signal enhancement. (B) Time course profiles of 23c-induced signal in brain regions. Profiles indicated by black triangles, gray circles, and open squares were obtained for ROI-c, -m, and -v defined on slice 3, respectively. Values are indicated by average ± SD of 2 mice.

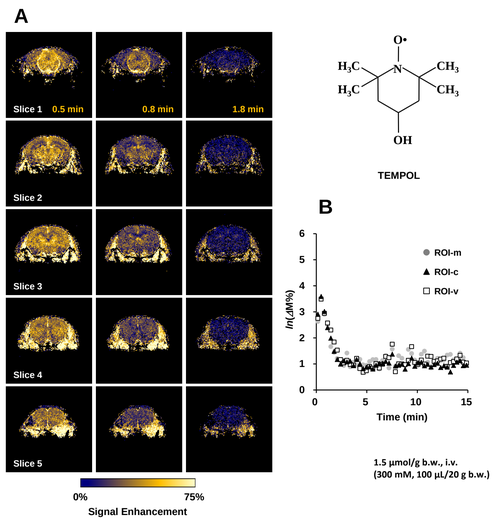

Fig. 8. Dynamic imaging of TEMPOL-induced T_1-contrast. (A) Distributions of TEMPOL in mouse brain and the time course. Vertical columns showed different slices of brain. Horizontal row showed the time course of the TEMPOL-induced T_1-signal enhancement. (B) Time course profiles of TEMPOL-induced signal in brain regions. Profiles indicated by black triangles, gray circles, and open squares were obtained for ROI-c, -m, and -v defined on slice 3, respectively. Values are indicated by average ± SD of 3 mice.

MC-PROXYL was chosen for the RedOx contrast agent of the subsequent experiments.

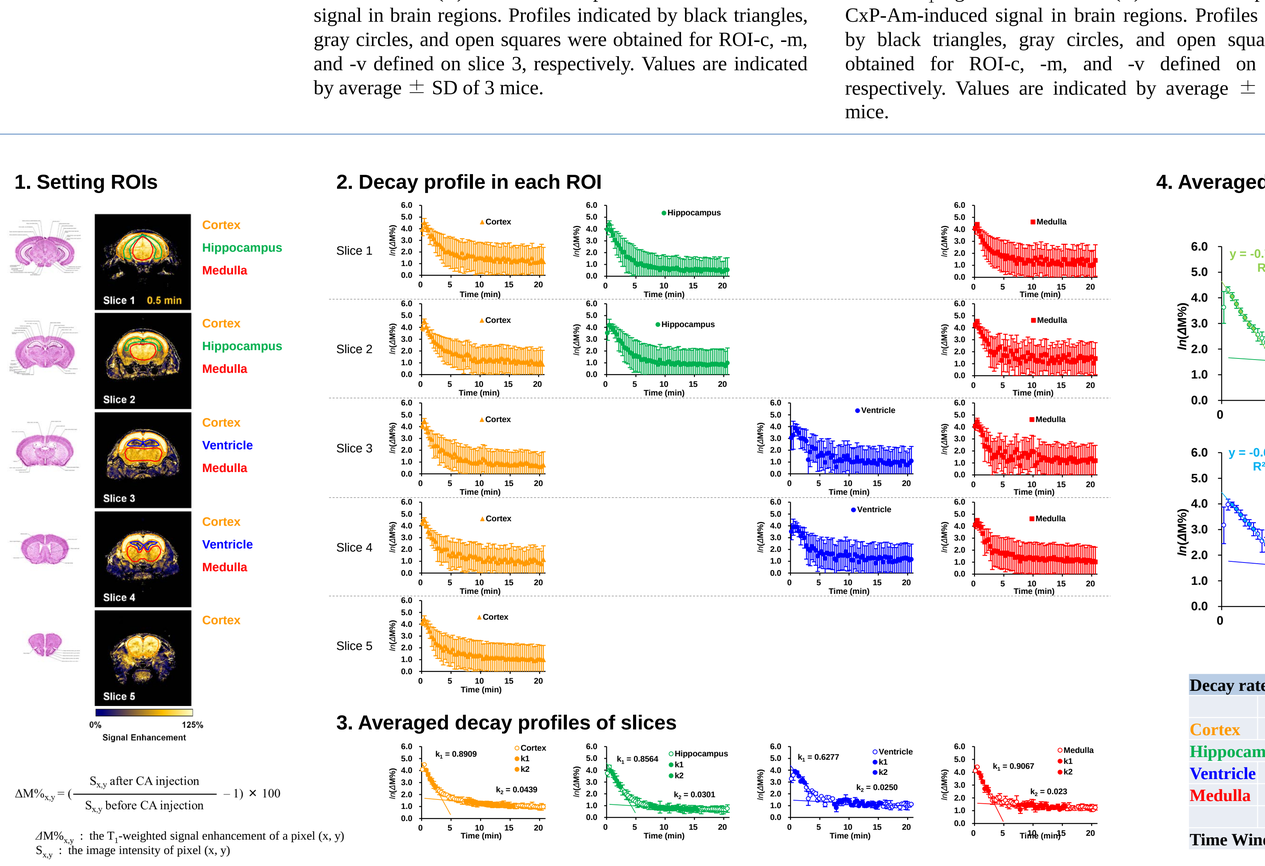

$$\Delta M\%_{x,y} = \left(\frac{S_{x,y} \text{ after CA injection}}{S_{x,y} \text{ before CA injection}} - 1\right) \times 100$$

$\Delta M\%_{x,y}$: the T_1-weighted signal enhancement of a pixel (x, y)
$S_{x,y}$: the image intensity of pixel (x, y)

Decay rates (min^{-1}) in different region in brain	k_1	SD	k_2	SD
Cortex	0.8488	0.1235	0.0459	0.0121
Hippocampus	0.7935	0.0972	0.0355	0.0146
Ventricle	0.6046	0.1072	0.0441	0.0165
Medulla	0.8980	0.1244	0.0308	0.0112
Time Window	0.8--2.4		7.5--15.5	

Healthy Unirradiated Control
C3H, Female, 8w
n = 9

Fig. 9. Process of Image Data Analysis for Subsequent Experiments. Decay rate k_1 mainly reflects reduction of the nitroxyl radical. Decay rate k_2 mainly reflects clearance of the nitroxyl radical.

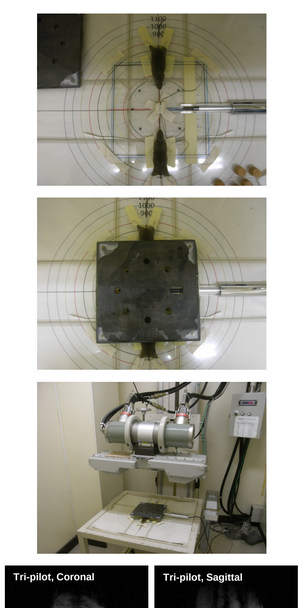

Fig. 10. Geometry of X-ray Irradiation.

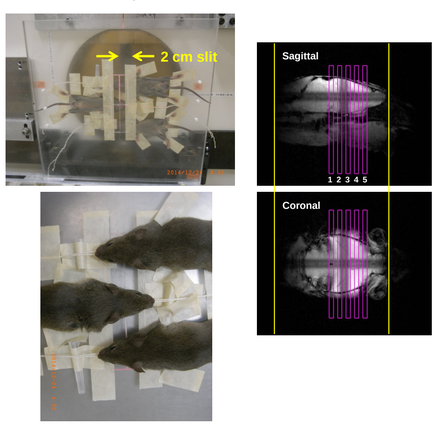

Fig. 11. Geometry of C-beam Irradiation.

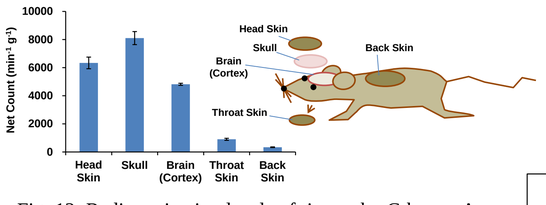

Fig. 12. Radio-activation levels of tissues by C-beam. An 8 Gy of 290 MeV carbon mono beam (LET = 60 keV/μm at the surface of the mouse) was irradiated. The radio activities were measured by a GM counter 30 min after irradiation.

X-ray, 8 Gy | C-beam, 8 Gy | C-beam, 16 Gy | C-beam, 8 Gy, TEMPOL

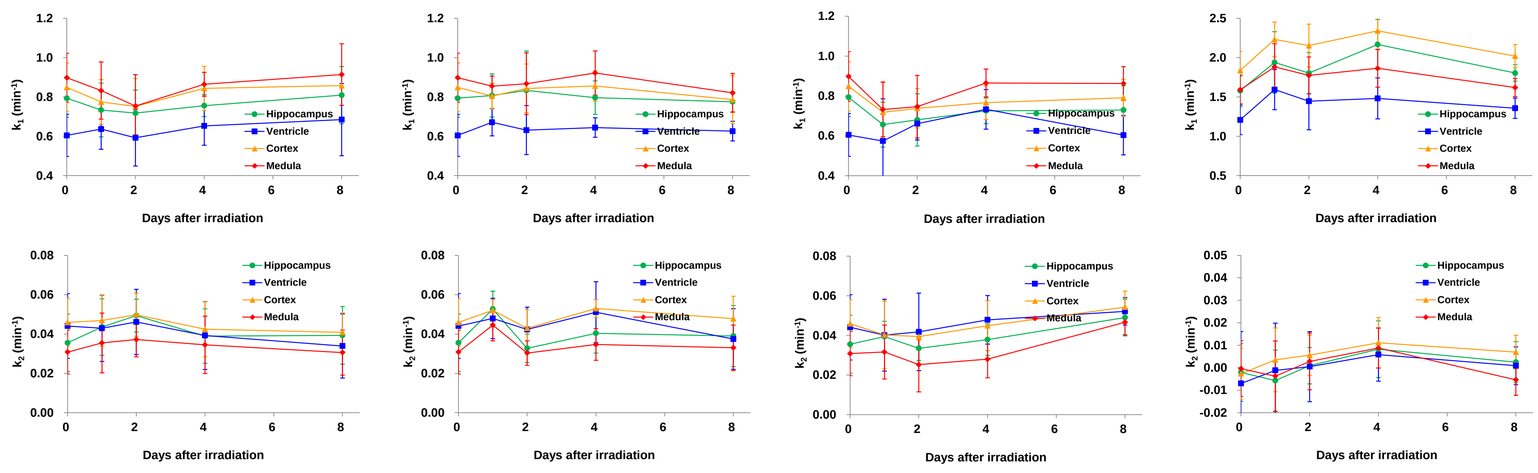

Fig. 13. Daily time courses of decay rates of MCP in regions of mouse brain after 8 Gy X-ray irradiation. Values are indicated by average ± SD of 9 mice.

Fig. 14. Daily time courses of decay rates of MCP in regions of mouse brain after 8 Gy C-beam (290 MeV mono beam, LET = 60 keV/μm at the surface of the mouse) irradiation. Values are indicated by average ± SD of 6 mice.

Fig. 15. Daily time courses of decay rates of MCP in regions of mouse brain after 16 Gy C-beam (290 MeV mono beam, LET = 60 keV/μm at the surface of the mouse) irradiation. Values are indicated by average ± SD of 6 mice.

Fig. 16. Daily time courses of decay rates of TEMPOL in regions of mouse brain after 8 Gy C-beam (290 MeV mono beam, LET = 60 keV/μm at the surface of the mouse) irradiation. Values are indicated by average ± SD of 6 mice.

- **For X-ray, alterations of RedOx status in the brain can be expected 2 days after the irradiation.**
- **For C-beam, alterations of RedOx status in the brain can be expected 1 day after the irradiation.**
- **The detail mechanisms of alterations of RedOx status in the brain were in progress.**